J Braz. Soc. Mech. Sci. Eng. (2017) 39:3269–3276
DOI 10.1007/s40430-017-0824-7

TECHNICAL PAPER

# Hybrid hill-type and reflex neuronal system muscle model improves isometric EMG-driven force estimation for low contraction levels

**Eduardo Lázaro Martins Naves[1] · Éder Alves de Moura[1] · Alcimar Barbosa Soares[1] · Liliam Fernandes de Oliveira[2,3] · Luciano Luporini Menegaldo[2]**

Received: 18 July 2016 / Accepted: 31 May 2017 / Published online: 12 June 2017


**Abstract** Non-invasive muscle force estimation by EMG signals can be obtained using a priori information provided by mathematical models of muscle dynamics. In this study, EMG-driven isometric force estimates performed using three muscle model formulations are compared to verify contribution of stretch reflex to muscle force estimation: (1) Winters' Hill-type model with muscle spindles and Golgi tendon organ reflex system; (2) Winters' model without reflex; and (3) Zajac model adapted by Menegaldo (ZM model). Submaximal isometric plantar flexion torque predictions, estimated by the models mentioned above, were compared with dynamometer measurements. Surface EMG was collected from *gastrocnemius medialis*, *gastrocnemius lateralis*, *soleus,* and *tibialis anterior* muscles from 12 volunteers and synchronized with dynamometer plantar flexion torque measurements. The experimental protocol consisted of sustained contraction intensities of 20 and 60% of individual maximum voluntary contraction (MVC) assisted by real-time visual feedback. The results show the improvement of torque prediction accuracy for the reflex model (1) at 20% MVC, which was not observed for 60% MVC.

**Keywords** Muscle model · Muscle reflex · EMG driven · Hill type · Muscle force prediction

## 1 Introduction

One of the fundamental problems in musculoskeletal biomechanics is estimating the muscle forces of different motor tasks. Mathematical models for muscle mechanics, such as Hill-type viscoelastic models, can be used for this purpose. Alternatively, microscopic models are based on cross-bridge mechanics, as proposed by Huxley [1]. Several muscle model formulations have been proposed after that in the literature [2–12].

Most of the studies mentioned above do not include the reflex feedback system in the control of muscle contraction. Naves [13, 14] used a muscle dynamics formulation that takes neural feedback reflexes into account. It is based on Winters' muscle-reflex model to simulate a standing posture [4, 5]. The model behavior was compared to data collected from an analogous situation with volunteers standing on a force platform. The results showed that the dynamic behavior predicted by the model was compatible with experimental data [15]. If used in forward dynamics simulations, reflex models are likely to improve low-intensity spring-like responses of equilibrium positions that occur in daily life activities such as walking or standing [5].

Electromyographic signals (EMGs) can be combined with muscle models to estimate in vivo muscle forces not invasively. This approach is known as EMG-driven modeling [16]. The EMG signal is rectified, low-pass filtered and normalized by the maximum voluntary contraction (MVC-EMG), generating an input signal to the muscle model. The ordinary differential equations of muscle mechanics are integrated numerically, resulting in a set of dynamic states.

Technical Editor: Estevam Las Casas.

✉ Eduardo Lázaro Martins Naves
eduardonaves@ufu.br

[1] Faculty of Electrical Engineering, Federal University of Uberlandia, Uberlândia, Brazil

[2] Biomedical Engineering Program, COPPE, Federal University of Rio de Janeiro, Rio de Janeiro, Brazil

[3] School of Physical Education and Sports, Federal University of Rio de Janeiro, Rio de Janeiro, Brazil

Such states include muscle forces. They are then multiplied by the respective moment arms, resulting in estimated joint torques. Such torques can be simultaneously measured by a dynamometer. Both estimated and measured torques can be compared [9]. This approach allows an indirect validation of the accuracy of muscle models.

Physiological feedback elements contribute significantly to muscle force generation at low contraction levels, such as standing upright, etc. [4, 5]. In the context of muscle biomechanics, motor tasks commonly investigated are frequently associated with moderated or high muscle contraction levels. In general, they are represented by an EMG envelope as input to muscle models.

The EMG envelope extraction procedure, which aims to determine muscle excitation, requires a digital low-pass filter with a very low cut-off frequency (see Sect. 2.2). A possible reason for the decrease in the accuracy of the EMG-driven model, at low force levels, may be related to a loss of neural drive information generated by reflexes. Such reflexes, as calculated by Winters' model, produce an additional excitation signal at low contraction levels which is likely to increase the excitation input to the EMG-driven model and attenuate the excessive filtering used for the extraction of the signal envelope. From the physiology point of view, the EMG signal already contains the reflex component; however, we have hypothesized that this strategy will work as feedforward controller, able to compensate for the low excitation error observed in [17], using a physiologically-based function.

The objective of this study is to evaluate whether the addition of reflex feedback components in muscle dynamics influences the accuracy of its force/torque prediction when using the EMG-driven model.

## 2 Materials and methods

### 2.1 Muscle models: basic description

Figure 1 shows a simplified block diagram of Winters' muscle-reflex model [4, 5]. Hill-type muscle models take only extrafusal fibers (EF) into account, while Winters' model includes the dynamic properties of intrafusal fibers (IF). Such fibers present muscular length sensors (muscle spindles) and are modeled similar to Hill-type muscle models, containing a contractile element (CE) and a series elastic element (SE). However, they work only as a length sensor that generates no contraction forces. The model also includes a Golgi tendon organ muscle force sensor. Signals from both sensors ($n_{sp}$ for spindle and $n_{gt}$ for Golgi) are a feedback to the spinal cord, resulting in the neural reflex signal $n_{rf}$, which modulates the descending efferent contraction command $n_{in}$, assumed here as the EMG envelope. Neural reflexes modulate the excitation level up to 10% of the Maximum Voluntary Contraction (MVC). The reflex is, therefore, able to compensate for small length variations (stretch) or force production [20] and is especially suitable for posture control simulations. The whole model has five first-order differential equations and dynamical states: excitation ($n_e$), activation ($n_a$), extrafusal contraction dynamics, intrafusal contraction dynamics, and attachment dynamics.

Excitation dynamics takes the feedback signals from muscle spindles, Golgi tendon organs, and Renshaw cells into account. Activation dynamics time constants vary in function of activation, while the Zajac model depends on excitation. The model also includes attachment dynamics, simulating force drops caused by a breakdown of cross-bridge bonds after stretch. Regarding the force–length relation, the maximum value for the active part shifts to the right (up to 20%) with a decreasing activation. The state variables of contraction dynamics are the lengths of series elastic elements (*SE*), both for extrafusal ($x_{se}$) and intrafusal ($x_{seif}$) fibers. Muscle force ($F_m$) is found by an exponential equation ($SE_T$) that takes into account the relation "toe" region of the *SE* force *x* length.

The neural feedback reflex signal is given by

$$n_{rf} = sp_k\left[n_{sp} - \frac{(n_{in} - n_r)}{2}\right] + gt_k\left(n_r - n_{gt}\right) + rc_k(n_r - n_e) \tag{1}$$

which depends on spindle ($n_{sp}$) and Golgi ($n_{gt}$) tendon organs reflexes:

$$n_{sp} = \frac{1}{sp_{rng}}\left[n_{sp_0} + sp_{kv}\frac{dn_{sp_0}}{dt}\right] \tag{2}$$

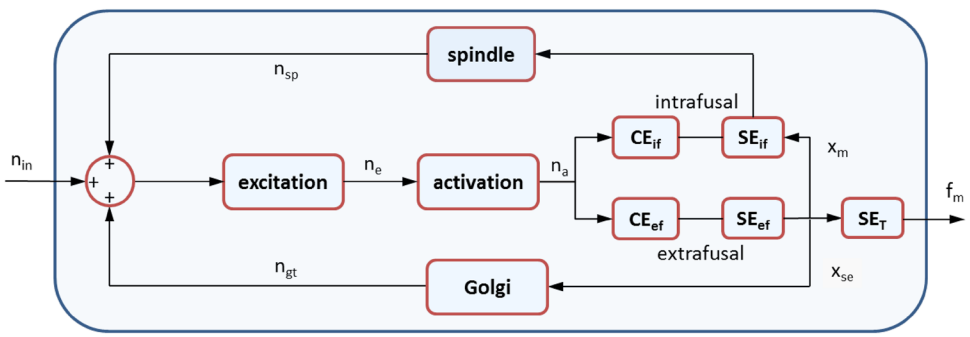


**Fig. 1** Simplified block diagram of the muscle-reflex model

$$n_{\mathrm{gt}} = \frac{1}{gt_{\mathrm{rng}}} e^{-\left[\frac{x_{\mathrm{se}} - gt_{oo}}{gt_{\mathrm{sh}}}\right]^2} \tag{3}$$

where $n_{\mathrm{sp}_0} = e^{-\left[\frac{x_{\mathrm{se-IF}} - sp_{oo}}{sp_{\mathrm{sh}}}\right]^2}$.

In the equations above, $sp_{\mathrm{k}}$, $gt_{\mathrm{k}}$, $rc_{\mathrm{k}}$, $sp_{\mathrm{kv}}$, $sp_{\mathrm{oo}}$, $gt_{\mathrm{oo}}$, $sp_{\mathrm{sh}}$, and $gt_{\mathrm{sh}}$ are the standard values for transducer gain and sensitivity, while $gt_{\mathrm{rng}}$ and $sp_{\mathrm{rng}}$ are physiological range values varying from 0.0 (strain representing zero firing) to 0.04 (peak sensor firing). To simulate the extrafusal-only Winters' model, $n_{\mathrm{rf}}$ is zeroed. For a sensitive analysis of Winters' model, see [8].

Menegaldo and Oliveira [9] formulated a Hill-Type EMG-driven musculotendon model based on Zajac [3] including parallel elastic and damping elements to improve numerical performance. This model is a modification of the Zajac model [3], which is mathematically simpler than Winters' and will be called Zajac's model modified by Menegaldo (ZM) from now on (Fig. 2). Therefore, as an intermediate step, the complexity of activation and contraction dynamics formulations will be increased (ZM to W-EF) and tested before including the reflex. Compared to Winters' model, it is similar to the extrafusal fibers part only although with a different formulation. The ZM model has been used in some publications, and its accuracy for torque estimation has been assessed experimentally [18]. The most relevant aspects of the Zajac model rely on a generic and non-dimensional set of variables and parameters, which can be defined for any skeletal muscle of the body. This model was the basis for the development of the SIMM (Software for Interactive Musculoskeletal Modeling) and its open-source counterpart, OpenSim [21], which is becoming a standard in musculoskeletal biomechanics modeling studies. According to Menegaldo and Oliveira [9], a muscle can be modeled using a system of three differential equations:

$$\begin{aligned} \dot{a} &= (u - a)(k_1 u + k_2) \\ \dot{\tilde{F}}^{\mathrm{T}} &= \tilde{k}^{\mathrm{T}}\left(\tilde{v}^{\mathrm{MT}} - \tilde{v}^{\mathrm{M}} \cos\alpha\right) \\ \dot{\tilde{L}}^{\mathrm{M}} &= \tilde{v}^{\mathrm{M}} \end{aligned} \tag{4}$$

where $a$ is neural activation, $u$ is excitation input signal, $k_1$ and $k_2$ are time constants, $F^{\mathrm{T}}$ is tendon force, $k^{\mathrm{T}}$ is tendon stiffness, $v^{\mathrm{MT}}$ is musculotendon velocity (an input variable), $v^{\mathrm{M}}$ is contractile element velocity, $\alpha$ is the pennation angle, and $L^{\mathrm{M}}$ is contractile element length. The ~superscript means that state variables are normalized and non-dimensional. The Hill hyperbole ($F^T \times v^M$) is scaled by activation level and force–length $F^M \times L^M$ scales of maximum muscle force. The first line of Eq. (4) is activation dynamics [22] and the second line represents contraction dynamics. The third is an auxiliary equation for explicitly integrate muscle velocity, obtaining muscle length to compute a force–length relation. Contraction dynamics requires expressing muscle velocity as an algebraic function of tendon force, activation, and muscle length.

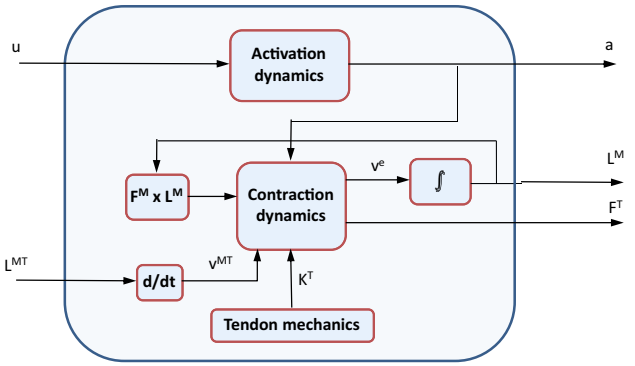


**Fig. 2** Simplified block diagram of the Zajac Hill-type model formulated by Menegaldo et al. (2009) (ZM model)

To evaluate the EMG-driven problem, the same processed EMG signals are considered as input both by Winters' ($n_{\mathrm{in}}$) and ZM ($u$) models, as described in the next section. In addition, aiming to maintain a compatibility between the models for comparison purposes, excitation and activation dynamics were included in all simulated models. In this way, it was guaranteed that reflex modeling was the only different characteristic between them. For the extrafusal part of Winters' model, both reflex and non-reflex versions, as well as the ZM model, musculotendon parameters from OpenSim two-legs model [21] were used. In this study, no scaling of parameters or subject-specific technique was applied. The parameters' list includes maximum isometric force, moment arm, tendon slack length, optimal muscle length, pennation angle, among others. Relative to the reflex part of the Winters' model, we adopted default values from [4].

## 2.2 Experimental setup

The isometric plantar flexion torque produced by the triceps surae muscle was chosen for the present study. Surface electromyography (EMG) signals were collected from 12 healthy young adult males. The experimental protocol was approved by the Ethics Committee of the University Hospital of the Federal University of Rio de Janeiro (Process no. 031/07 HUCFF).

Subjects laid prone on a Norm/Cybex™ Dynamometer, with knees extended and the ankle at the neutral position (90°) (Fig. 3). The right foot was firmly fixed to the foot adaptor. The familiarization session consisted of submaximal plantar flexion contractions followed by one maximal effort and step trials. The isometric plantar flexion torque

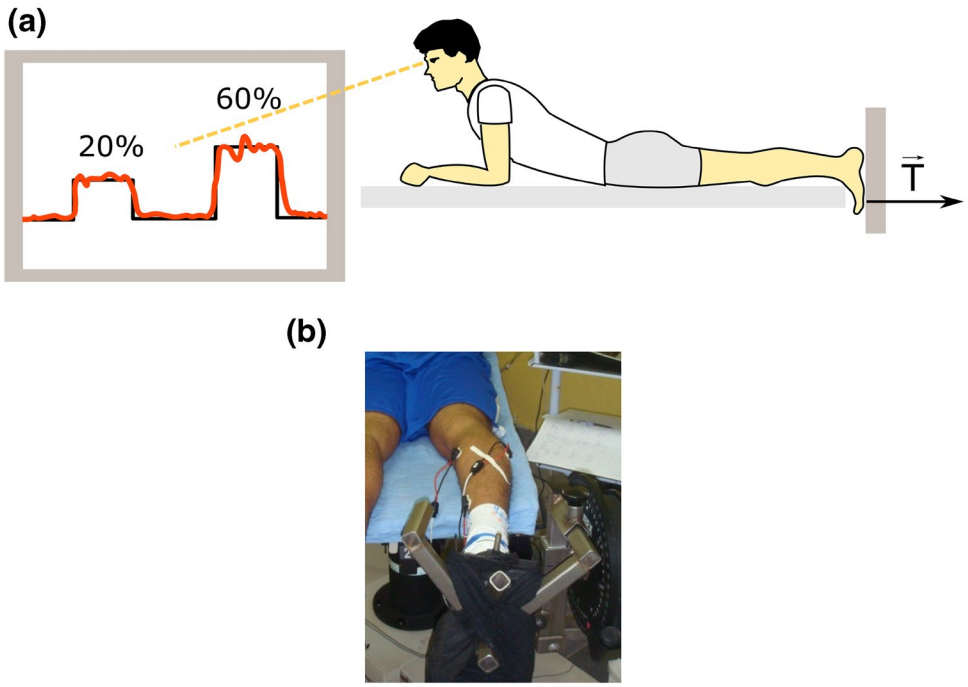


**Fig. 3** Position of the subject on the experimental set. **a** Visual feedback with the actual ankle torque superimposed to a mask with the desired torque is shown to the subject. **b** Position of the EMG electrodes on the *triceps surae*

associated with the MVC was collected during 5 s twice, with a 2-min rest between tests. The highest value was selected as the maximum subject torque. Each volunteer was instructed to follow a protocol consisting of two 10-s steps with submaximal isometric loads of 20 and 60% of the individual MVC, separated by 30-s relaxing intervals. This contraction range represents two different strategies of the nervous system to control muscle force. In 20% MVC, raising the motor unities (MUs) recruitment rate is the preferable strategy. On the other hand, at 60% MVC, approximately all MUs are already recruited, and the firing rate becomes the control option [23]. The intermediary levels of MVC represent these two strategies in different extends.

A feedback display of the actual torque output was provided to the subject, who attempted to match it to a masking protocol. Torque signal and surface EMG were synchronously collected using an electromyographic equipment (EMG 800C—EMGSystem™, Brazil), with a common-mode rejection ratio (CMRR) of 106 dB, an analogical band-pass filter of 10–500 Hz, a 2 kHz sampling rate, and 16 bits A/D converter. Ag/AgCl pre-gelled bipolar electrodes were positioned on the *gastrocnemius medialis* (GM), *gastrocnemius lateralis* (GL), *soleus* (SOL), and *tibialis anterior* (TA) muscles, according to SENIAM recommendations [24], after skin preparation. The reference electrode was positioned on the left lateral malleolus.

The digitized EMG signal from each muscle was initially band-pass filtered (10–350 Hz) to remove artifacts, then rectified, and low-pass filtered with a second-order Butterworth filter (2 Hz cut-off frequency). EMG-driven models require the normalization of the input signal by the mean EMG value obtained during 1 s of MVC torque x time curve when the maximal torque was achieved. Hence, the resulting envelope signal was normalized by the maximum value of the EMG-MVC signal and considered as the excitation input for all experimented muscle models.

### 2.3 Simulation of EMG-driven models

The analysis has been carried out using the muscle-reflex model proposed by Winters [4, 5]. It was simulated in two situations using the same set of EMG data: (1) without reflex feedback, working as a Hill-type muscle model (Winters' extrafusal model—W-EF) and (2) with reflex feedback, providing a reflexive model (Winters' intrafusal model—W-IF). The EMG signal is directly related to the α-motoneuron activity, which is an output for spinal cord feedback computation based on the reflex information. In addition, we compared the torque prediction accuracy of Winters' formulations to our own Hill-type muscle model as performed in the previous works [9], which does not include reflex.

The excitation signal is considered as an input to muscle differential equations. The equations were converted to Simulink Blocks and integrated numerically using a third-order Runge–Kutta Matlab/Simulink R2009a implementation (Core 2 Duo P8600 2.4 GHz, 4 GB RAM, Windows 7). Integration step size was fixed at 0.0005 s, which is compatible with the EMG sampling. The simulation time was approximately 60 s per running. The force

produced by a muscle and transmitted by its tendon is a function of maximum muscle force, excitation input, initial conditions, muscle length, degree of activation, pennation angle, and several other anatomical and functional parameters [9]. If the muscle is excited to the maximum, the highest tendon force will be produced regarding the actual muscle length, velocity, and additional operating conditions. One must be aware that, despite only isometric contractions are being addressed here, the muscle contractile element shortens at the expense of the lengthening of the respective tendon to keep the musculotendon length the same. The torque output can be determined by summing each simulated muscle force multiplied by its respective ankle angle moment arm, as presented by Eq. (5):

$$\begin{aligned} T_{\text{Total}} &= r_{\text{GM}}F_{\text{GM}} + r_{\text{GL}}F_{\text{GL}} + r_{\text{SOL}}F_{\text{SOL}} - r_{\text{TA}}F_{\text{TA}} \\ &= T_{\text{GM}} + T_{\text{GL}} + T_{\text{SOL}} - T_{\text{TA}} \end{aligned} \tag{5}$$

where $T_{\text{Total}}$ is total ankle torque, $r_{\text{GM}}$, $r_{\text{GL}}$, $r_{\text{SOL,}}$ and $r_{\text{TA}}$ are ankle joint moment arms of GM, GL, SOL, and TA, respectively, and forces $F_{\text{GM}}$ etc. and muscle torques $T_{\text{GM}}$ etc.

The simulation was divided into two stages. First, the extrafusal part of the Winters' model was isolated and simulated, resulting in a typical Hill-type muscle model. Second, extrafusal and muscle-reflex (extrafusal + intrafusal) Winters' models were implemented and tested.

For the first stage, the activation signal $n_{\text{a}}$, obtained by the rectified and normalized EMG ($n_{\text{in}}$), was assumed as the input signal for the W-EF model (see Fig. 1). The same signal was used to integrate the ZM model. To evaluate the role of the reflex system, the W-IF model was simulated with inputs from both EMG signal envelopes considered in the first stage and the components generated by reflex system modulations, which depend on the feedback from the Golgi tendon and spindle sensors.

The concordance between torque curves measured by the dynamometer and curves estimated by each EMG-driven model was evaluated by the Root Mean Square Error (RMSE) between the two curves:

$$\%\text{RMSE} = \frac{1}{\text{TM}_{\text{MAX}}}\sqrt{\frac{\sum_{i=1}^{N}(\text{TM}(i) - \text{TS}(i))^2}{N}} \times 100\% \tag{6}$$

where TM is dynamometer-measured torque, TS is simulated torque, $N$ is number of samples in the time series, and $\text{TM}_{\text{MAX}}$ is maximum torque measured by the dynamometer at MVC for each subject.

The differences in the average %RMSE among ZM, W-EF, and W-IF, for each step contraction, were analyzed using ANOVA with repeated measures and Tukey's post hoc test. Differences between each model for 20 and 60% MVC were tested using the Wilcoxon test after verifying normality using the Shapiro–Wilk test at a 95% ($p = 0.05$) significance level.

## 3 Results

The root mean square error (%RMSE) between torques estimated by the dynamometer-measured and EMG-driven model is shown in Table 1 for 20 and 60% of MVC contraction intensity. All RMSEs from the three models at 20% MVC were significantly lower than the respective values for the 60% MVC step ($p = 0.0005$).

**Table 1** %RMSE of ankle torque estimates between dynamometer-measured and model-estimated

| Subject | 20% MVC | | | 60% MVC | | |
|---|---|---|---|---|---|---|
| | ZM | W-EF | W-IF | ZM | W-EF | W-IF |
| 1 | 6.84 | 8.04 | 5.67 | 9.54 | 15.79 | 44.52 |
| 2 | 2.53 | 3.34 | 2.75 | 8.66 | 21.35 | 55.90 |
| 3 | 6.56 | 8.12 | 6.71 | 14.99 | 29.52 | 53.64 |
| 4 | 13.28 | 14.53 | 11.31 | 16.54 | 14.77 | 18.71 |
| 5 | 6.57 | 7.79 | 5.77 | 24.49 | 20.49 | 11.92 |
| 6 | 18.31 | 18.50 | 16.00 | 48.83 | 47.20 | 40.45 |
| 7 | 17.41 | 18.99 | 15.58 | 21.31 | 21.06 | 12.73 |
| 8 | 10.19 | 10.02 | 7.34 | 17.00 | 13.30 | 31.51 |
| 9 | 12.68 | 13.67 | 10.85 | 36.29 | 34.57 | 23.81 |
| 10 | 19.08 | 20.53 | 17.53 | 51.74 | 53.92 | 48.83 |
| 11 | 4.64 | 4.62 | 5.46 | 11.03 | 14.42 | 26.66 |
| 12 | 7.28 | 7.86 | 5.87 | 15.18 | 12.99 | 27.84 |
| Mean ± SD | 10.44 ± 5.62 | 11.33 ± 5.77 | 9.23 ± 4.89 | 22.96 ± 14.79 | 24.94 ± 13.72 | 33.04 ± 15.38 |

*ZM* Zajac/Menegaldo model, *W-EF* Winters' model, extrafusal-only, *W-IF* Winters' model, muscle reflex

The error levels associated with the 20% MVC contraction were statistically different among the tree models ($p = 0.0001$). W-IF was the best torque predictor. The ZM model resulted in significantly reduced errors when compared to W-EF ($p < 0.05$).

At 60% of MVC, the RMSE was similar among models. In Fig. 4, it is possible to observe a sample (one subject) of the torque measured by the dynamometer (continuous gray line) and the estimates from ZM and W-EF models. Figure 5 shows a graphical comparison of the measured torque and the estimates for the W-IF and W-EF models, also for one subject.

## 4 Discussion

The discussion evolves to determine whether introducing the reflex feedback (W-IF) could provide better muscle force estimations. Our group has extensively used the ZM model in numerous EMG-driven model studies [18], and the comparison with the performance of Winters' model will be helpful to assess whether this model is still valid or should be replaced by a more sophisticated model such as Winters' model. The comparison between the two extrafusal models (ZM and W-EF) resulted in an approximately 11% error, with a better relative accuracy for 20%

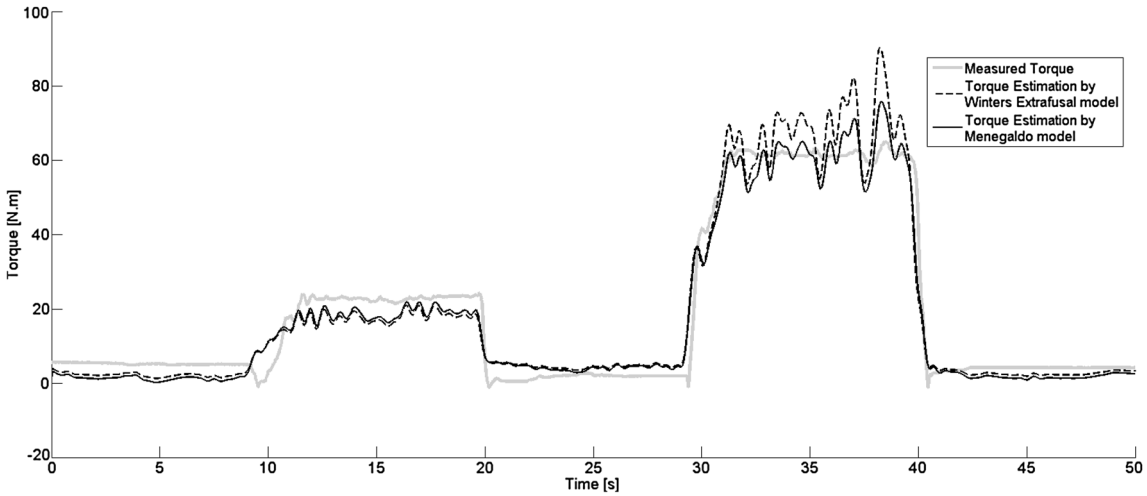


**Fig. 4** Measured torque and estimations from the extrafusal-only muscle models: Winters' (W-EF) and Zajac/Menegaldo (ZM) models

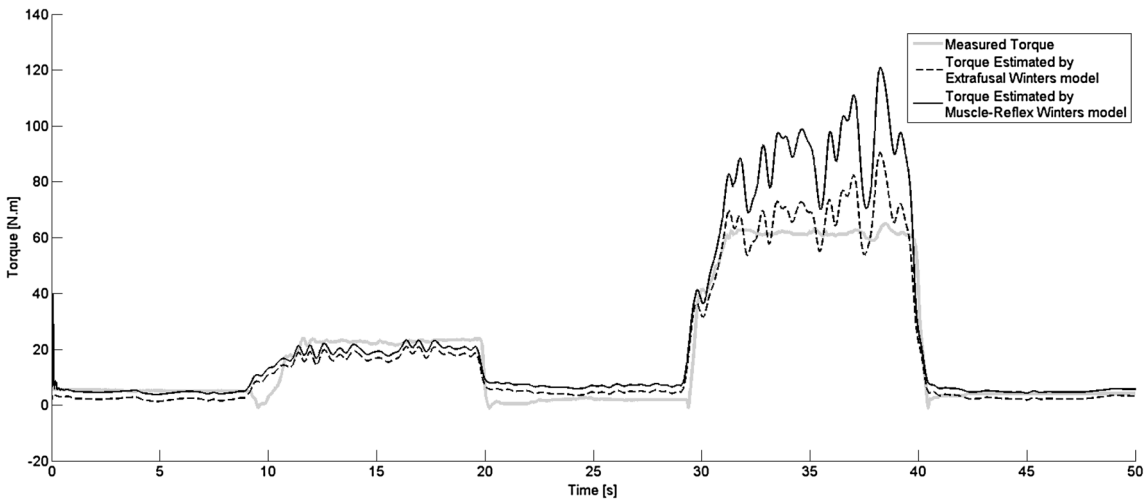


**Fig. 5** Measured torque and estimates from reflex (W-IF) and non-reflex (W-EF) Winters' models

MVC when compared to the 60% MVC (all comparisons between intensities for the three model versions had $p < 0.05$). The ZM model was most accurate. In Fig. 4, it is possible to observe that the estimated torque curves of the models oscillate around the dynamometer-measured curve. However, the W-EF model presented greater oscillation amplitudes when compared to the ZM model. For the reflex model (W-IF), the accuracy of torque estimation increased by approximately 2% about the W-EF for the 20% MVC step. For 60% MVC, statistically equivalent error levels were observed for W-EF, W-IF, and ZM (Fig. 5).

An increase in statistical accuracy was observed when the reflex system was included in the low-level activation case (20% MVC). This was not observed for 60% MVC, which is an interesting finding. Actually, the reflex system plays a significant role in lower levels of muscle activation related to postural control reflexes [4]. For greater activation levels, the relative contribution of the reflex system is expected to decrease progressively [25]. This is also in line with classic studies that documented in detail how open-loop muscle behavior differs from systems that include autogenic reflex activity, especially for small force levels [26]. Therefore, the closed-loop reflex formulation presented here should be considered primarily for force estimation of small muscle contraction levels. Regarding the numerical behavior, no significant increases in computational cost or numerical instability were observed for the reflex model.

The apparent drift related to the dynamometer measurement, shown in Figs. 4 and 5, can be associated with the remaining passive plantar flexor torque when the ankle is in neutral position [27]. The amount of muscle actuation provided by reflex mechanisms is likely to increase in a joint neutral position [25], which was adopted here. Thus, for model estimation, the residual torque can be associated with the EMG activity of the remaining muscle tonus. Some limitations of this analysis should be pointed out. Bipolar EMG is prone to several sources of errors [28]. No technique to adjust individual muscular parameters was used, only literature average values. Only two levels of isometric contractions were analyzed. The contribution to the plantar flexor torque by muscles other than triceps surae was not considered. Because they are deep muscles, the access to them by EMG would require an invasive EMG. The small foot displacement provided by the fixing dynamometer apparatus and the deformation of body soft tissue and dynamometer seat cushion was not considered. Regarding the applicability of the reflex model, when muscle activity is high, the estimation of force becomes less accurate than the extrafusal-only model. For improving force estimation accuracy, from the limitations mentioned above, obtaining subject-specific parameters, from medical imaging, functional tests, scaling, etc. is the most efficient way [19].

## 5 Conclusion

It was possible to observe that, for low-level muscle activation, reflex contributes to a more accurate muscle force estimation based on simulations of the Winters' reflex model for the *triceps surae* in studies on EMG-driven model when compared to the extrafusal-only Hill-type models simulated here. Such increase in accuracy has been inferred indirectly from isometric ankle torque curves measured with the ankle in the neutral position. This study points towards a possible direction for a new, hybrid and more realistic muscle model incorporating the reflex system, being the dependence on the reflex action a function of muscle activation level. Such model would be based on ZM contraction dynamics, which has shown to be more accurate than W-EF. However, the reflex part from W-IF would be incorporated. In this case, Eqs. (2) and (3) should be multiplied by a shape factor that decreases with increasing activation level.

## References

1. Huxley AF (1957) Muscle structure and theories of contraction. Prog Biophys Biophys Chem 7:255–318
2. Huxley HE (1969) The mechanism of muscular contraction. Science 164(3886):1356–1366
3. Zajac FE (1989) Muscle and tendon: properties, models, scaling, and application to biomechanics and motor control. Crit Rev Biomed Eng 17(4):359–411
4. Winters JM (1995) An improved muscle-reflex actuator for use in large-scale neuromusculoskeletal models. Ann Biomed Eng 23(4):359–374
5. Winters JM (1995) How detailed should muscle models be to understand multi-joint movement coordination? Hum Mov Sci 14(4–5):401–442
6. Rosen J, Fuchs MB, Arcan M (1999) Performances of Hill-type and neural network muscle models—toward a myosignal-based exoskeleton. Comput Biomed Res 32(5):415–439
7. Staudenmann D, Potvin JR, Kingma I, Stegeman DF, van Dieën JH (2007) Effects of EMG processing on biomechanical models of muscle joint systems: sensitivity of trunk muscle moments, spinal forces, and stability. J Biomech 40(4):900–909
8. Winters JM, Stark L (1985) Analysis of fundamental human movement patterns through the use of in-depth antagonistic muscle models. IEEE Trans Biomed Eng BME 32(10):826–839
9. Menegaldo LL, Oliveira LF (2009) Effect of muscle model parameter scaling for isometric plantar flexion torque prediction. J Biomech 42(15):2597–2601
10. Röhrle O, Davidson JB, Pullan AJ (2012) A physiologically based, multi-scale model of skeletal muscle structure and function. Front Physiol 3:358
11. Hayashibe M, Guiraud D (2013) Voluntary EMG-to-force estimation with a multi-scale physiological muscle model. BioMed Eng OnLine 12:86
12. Weickenmeier J, Itskov M, Mazza E, Jabareen M (2014) A physically motivated constitutive model for 3D numerical simulation of skeletal muscles. Int J Numer Methods Biomed Eng 30:545–562

13. Naves ELM (2006) Modelagem e simulação do controle da postura ereta humana quasi-estática com reflexos neuromusculares. Ph.D. Thesis. Federal University of Uberlandia, Brazil (in Portuguese)
14. Naves ELM, Soares AB, Pereira AA, Andrade AO (2007) Modelagem do controle neuromuscular da postura ereta quasi-estática humana. Rev Bras Biomec 8:1–9
15. Pereira AA, Naves ELM, Andrade AO, Cavalheiro G., Rocha LAA, Moraes NN (2010) Otimização de parâmetros de um controlador PID referente a um novo modelo de controle postural humano. XVIII Congresso Brasileiro de Automática, pp 1694–1699
16. Lloyd DG, Besier TF (2003) An EMG-driven musculoskeletal model to estimate muscle forces and knee joint moments in vivo. J Biomech 36:765–776
17. Perreault EJ, Heckman CJ, Sandercock TG (2003) Hill muscle model errors during movement are greatest within the physiologically relevant range of motor unit firing rates. J Biomech 36(2):211–218
18. Oliveira LF, Menegaldo LL (2012) Input error analysis of an EMG-driven muscle model of the plantar flexors. Acta Bioeng Biomech 14:75–81
19. Menegaldo LL, Oliveira LF (2012) The influence of modeling hypothesis and experimental methodologies in the accuracy of muscle force estimation using EMG-driven models. Multibody Syst Dyn 28:21–36
20. Windhorst U (2007) Muscle proprioceptive feedback and spinal networks. Brain Res Bull 73:155–202
21. Delp SL, Anderson FC, Arnold AS, Loan P, Habib A, John C, Guendelman E, Thelen DG (2007) OpenSim: open-source software to create and analyze dynamic simulations of movement. IEEE Trans Biomed Eng 54:1940–1950
22. Piazza SJ, Delp SL (1996) The influence of muscles on knee flexion during the swing phase of gait. J Biomech 29:723–733
23. De Luca CJ, LeFever RS, McCue MP, Xenakis AP (1982) Behaviour of human motor units in different muscles during linearly varying contractions. J Physiol 329:113–128
24. Hermens HJ, Freriks B, Merletti R, Stegeman D, Blok J, Rau G, Hägg G (1999) European recommendations for surface electromyography. Roessingh Res Dev 8(2):13–54
25. Mirbagheri MM, Barbeau H, Kearney RE (2000) Intrinsic and reflex contributions to human ankle stiffness: variation with activation level and position. Exp Brain Res 135:423–436
26. Hoffer JA, Andreasson S (1981) Regulation of soleus muscle stiffness in premammilary cats: intrinsic and reflex components. J Neurophys 45:267–285
27. Souza TR, Fonseca ST, Gonçalves GG, Ocarino JM, Mancini MC (2009) Prestress revealed by passive co-tension at the ankle joint. J Biomech 42(14):2374–2380
28. Farina Dario, Cescon Corrado, Merletti Roberto (2002) Influence of anatomical, physical, and detection-system parameters on surface EMG. Biol Cybern 86(6):445–456